Synthesis and Electrochemical Performance of $Li_xMn_{2-y}Co_yO_{4-d}Cl_d$ Cathode Material

Terrill B. Atwater, Paula C. Latorre, and Ashley L. Ruth

U.S. Army, Aberdeen Proving Ground, MD

Abstract: *Lithium manganese oxide spinel is a potential candidate for Li-ion battery cathodes because of its low toxicity, comparable capacity, and low cost. However, this spinel suffers from capacity fading due to fracturing of the cell structure. Historically, cycle life enhancements of spinels have been achieved through transition metal doping on the "B" site of the lattice. In this effort, dopants of interest include compounds containing Group VIII Row 4 (Fe, Co, and Ni) elements, cobalt in particular. In addition to fabrication method variants of this material, the electrochemical performance and cycle life data of the Co "B" site and Cl "O" site manganese-based AB_2O_4 spinel is presented in this paper. Lithium electrochemical cells with Co "B" and Cl "O" site doping of a Mn-based AB_2O_4 spinel cathode have demonstrated the following: 1) full reversibility between 4.5 V and 2.0 V, 2) low charge/discharge overpotential between 4.5 V and 3.5 V, 3) high specific capacity of 240 mAh/g of active material, and 4) high rate charge and discharge.*

Keywords: Lithium and Li-ion battery, Lithium manganese oxide spinel, Spinel cathode, Co-doping, Cl-doping

Introduction

The benefits of lithium battery systems lie within their high energy density (Wh/L) and high specific energy (Wh/kg). Manganese dioxide (MnO_2) is an attractive active cathode material because of its high energy density and low material cost. Manganese dioxide is an intercalating compound for lithium that functions by solvating and desolvating lithium cations from the electrolyte in solid state. The lithium cations are deposited into the vacancies of the MnO_2 cathode crystal structure. The objective of this effort focuses on the limited cycle life of rechargeable lithium manganese-based electrochemical systems, namely capacity fading of the cathode. These two characteristics are considered the major technical hurdles in rechargeable lithium battery technologies.[1-4]

Background

Capacity fading is the loss of cycle capacity in a cell over the entire life of a battery system, limiting the practical number of cycles that may be used. In lithium battery systems, capacity loss is often attributed to the degradation of the active cathode material. This degradation is a result of changes in both composition and crystal structure of the active material that occur during charging and discharging of the cell. The crystal structure of the active material changes in coordination with the state of charge of the cell. This is linked to intercalation of lithium cations into the active material. Additionally, throughout the life of a cell, parasitic side reactions occur between the chemical species of the cell components. These include chemical dissolution and degradation of the active cathode material. Methods reducing this effect include changing the crystal structure and composition of the active material or eliminating these parasitic mechanisms through other means. Capacity fading is currently a major setback for rechargeable lithium cells and is therefore an active area of research.[2-9]

Manganese dioxide exists in different phase states or crystal structures. The common phases are referred to by the following prefixes: α, β, γ, and λ. α-MnO_2 is the most stable structure; it is a one-dimensional lattice containing both one-by-one, and two-by-two channels for lithium insertion/extraction. γ-MnO_2 is a one dimensional structure but has a one-by-two channel. λ-MnO_2 is created through the delithiation of Li-Mn-O type spinels ($Li_xMn_2O_4$). The crystal structure of the spinel is maintained through both delithiation and lithiation. The λ crystal structure is a three-dimensional cubic array. This structure promotes mechanical stability and adequate pathways for lithium insertion/extraction. λ-MnO_2 is perhaps the most preferred rechargeable phase on MnO_2. Degradation of the λ-MnO_2 crystal structure, forming α/γ-MnO_2 and other Mn_xO_y phases, reduces the capacity of the cathode material.[10-17]

A family of halogenated "B" site doped $AB_2O_{4-d}X_d$ lithium manganese spinel materials was synthesized and evaluated as a cathode for lithium and lithium-ion electrochemical systems. This spinel is formulated with the general stoichiometry $Li_xMn_2O_{4-d}X_d$, where $x \approx 1$ and d ranges from 0.005 to 0.3; this work was reported previously and also demonstrated in these current proceedings.[18-20] By introducing halogens into the starting material mixture and thereby into the final product, the synthesis process time of lithium manganese-based AB_2O_4 spinel materials is dramatically reduced. Additionally, when coupled with a lithium anode, the $Li_xMn_2O_{4-d}X_d$ material proved to be reversible to voltages as low as 2.0 V (where x is approaching 2). In order to stabilize the manganese to improve cycle life, Group VIII Period 4 elements (Fe, Co, Ni) were doped into the "B" site. This paper will present data relating to the Co-doped material while the Fe-doped material is presented in a complementary paper in these proceedings.

Experimental

A glycine nitrate combustion method was used to synthesize cobalt-doped chlorinated lithium manganese oxide spinel. Stoichiometric amounts of $Li(NO_3)$ and $Mn(NO_3)_2{\cdot}4H_2O$ and $Co(NO_3)_2{\cdot}4H_2O$ (Alfa Aesar) with $MnCl_3$ were mixed and then dissolved in distilled water. NH_2CH_2COOH (glycine, Alfa Aesar) was dissolved into the aqueous solution as a chelating agent in a 1:1 metal ion-to-glycine ratio. The solution was heated to 80 °C until the water fully evaporated and a gel was formed. The gel was heated further to 250 °C when auto ignition occured and formed metallic oxide ash. The ash was collected and ground in a mortar and pestle and fired at 600 °C for two to six hours to achieve the desired phase.

The $Li_xMn_{2-y}Co_yO_{4-d}Cl_d$ material was also fabricated using a solid state process where manganese and cobalt mixed metal oxides along is combined with Li_2CO_3 or LiOH as the principal starting material. Halogens were introduced into the starting material mixture and subsequent final product using lithium halide salts. The subsequent material mixture was ground using a random orbit mixer mill and was then heated at 600 ^oC in air.

Phase purity was determined using X-ray diffraction (XRD, Bruker D8 Advance, Cu-kα). Samples of $LiMn_2O_4$ (non-doped and non-chlorinated lithium manganese oxide) were synthesized via the above mentioned process without the halogen or Group VIII addition to determine structure changes that occurred. Both chlorine-to-manganese and Group VIII-to-manganese stoichiometry was determined from X-ray fluorescence spectroscopy (XRF, Bruker S2 Ranger). An Olympus metallograph was used to observe the morphology of the particles.

The experimental cells were composed of a lithium anode separated from the cathode by a nonwoven glass separator. The $Li_xMn_{2-y}Co_yO_{4-d}Cl_d$ cathode was fabricated by mixing together the active material, carbon, and polytetrafluoroethylene in an 85:10:5 by weight ratio, respectively. The cathode mixture was rolled to 0.04 cm and dried in a vacuum oven. A 0.075 cm thick lithium foil was cut using a 19.0 mm diameter hole punch. The cathode was cut into 2.85 cm^2 discs, resulting in a 0.13 g cathode. A 0.01 cm nonwoven glass separator was utilized for the separator and as a wick. The electrolyte used was 1 molar $LiPF_6$ in proportional mixtures of diethyl carbonate, dimethyl carbonate, and ethylene carbonate.

Cells were cycled with an ARBIN MSTAT4 battery cycler system controlled by MITS Pro software. The cells were charged and discharged from 4.5 V to 3.5 V, 4.5 V to 2.25 V, or 4.75 V to 3.5 V. The charge/discharge rates were maintained at 1.0 mA/cm^2 or 2.0 mA/cm^2. A rest period of 15 minutes between charge and discharge cycles was used to allow for cells to achieve equilibrium on all experiments.

Results

After formulation of the $Li_xMn_{2-y}Co_yO_{4-d}Cl_d$ material, the physical properties were evaluated using powder X-ray diffraction. The stoichiometry was verified with X-ray fluorescence. Figure 1 shows the X-ray diffraction pattern for a family of $Li_xMn_{2-y}Co_yO_{4-d}Cl_d$, where $x \approx 1$ and y ranges from 0.05 to 0.2 (bottom to top pattern). These patterns are representative for both the chlorinated and fluorinated $AB_2O_{4-d}X_d$ material. The undesirable Mn_2O_3 product was minimized by maintaining a slight $x > 1$ lithium stoichiometry.

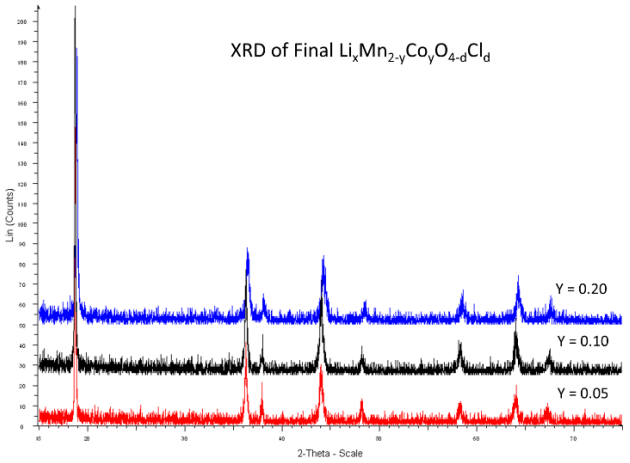

Figure 1. The X-ray diffraction pattern for a family of $Li_xMn_{2-y}Co_yO_{4-d}Cl_d$ where x ≈ 1 and y ranges from 0.05 to 0.2.

In addition to identifying the resultant $Li_xMn_{2-y}Co_yO_{4-d}Cl_d$ spinel material, Figure 1 also shows a slight shift to higher 2-theta values (smaller d-spacing) with increasing cobalt concentrations as expected from the smaller ionic radius of cobalt versus manganese.

Figures 2-5 show the electrochemical characterization of the $Li//Li_xMn_{2-y}Co_yO_{4-d}Cl_d$ couple. Figures 2 and 3 show charge/discharge data displayed as a hysteresis plot and a differential capacity plot, respectively. These figures show the initial formation cycles for the $Li//Li_xMn_{2-y}Co_yO_{4-d}Cl_d$ electrochemical system. The reversible region for the $Li//Li_xMn_{2-y}Co_yO_{4-d}Cl_d$ electrochemical couple occurs where $0.25 < x < 1.80$ in a three-step thermodynamic charge/discharge profile. Figure 2 shows the high capacity capability approaching 240 mAh/g.

The figures reveal that a small portion of the low voltage (down to 2.25 V) discharge process is recharged at an elevated voltage rather than centered about the 2.9 V; Figures 2 and 3 show the corresponding charge peak at 3.65 V. The high voltage plateau is a pair of twin peaks centered on a 4.14 V and 3.99 V potential (4.11 V and 3.97 V for discharge) and the low voltage plateau is centered on a 2.95 V potential (2.81 V for discharge). The data displayed in the figures show the

charge/discharge data at a slow, 100-hour rate, revealing the kinetic and thermodynamic properties of the system. The differential capacity curves show the low overpotential required for charge at the upper plateau, which is on the order of 0.05 V. The overpotential for charge at the low voltage thermodynamic region is on the order of 0.15 volts.

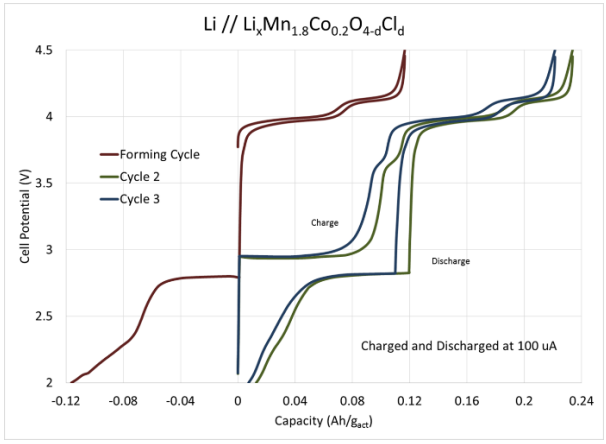

Figure 2. Galvanostatic data, displayed as a hysteresis graph (charge/discharge) of a representative Li//$Li_xMn_{2-y}Co_yO_{4-d}X_d$ electrochemical cell showing the formation cycle.

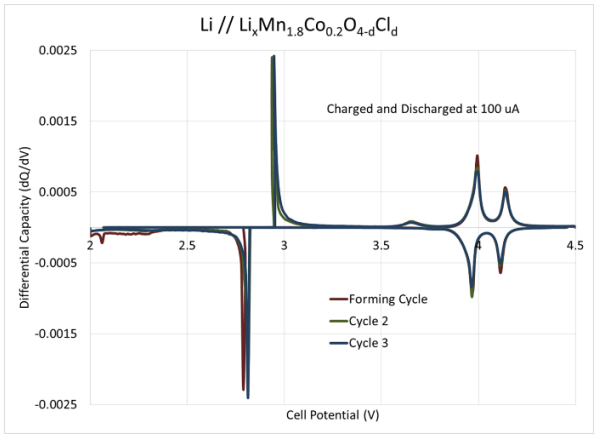

Figure 3. Galvanostatic data displayed as a differential capacity graph for a representative Li//$Li_xMn_{2-y}Co_yO_{4-d}X_d$ electrochemical cell showing the formation cycle.

Figures 4 and 5 display the charge/discharge data of a representative cell showing the thermodynamic stability of the Li//$Li_xMn_{2-y}Co_yO_{4-d}X_d$. Charge and discharge cycles were performed after cells were stored at various conditions and after repeated deep discharge cycling to 2.25 V. Storage included the following conditions: 1) 55 ºC for 4 weeks on an unformed (as assembled) cell, 2) 55 ºC for 4 weeks on a cell discharged to 3.5 V, 3) 20 ºC for 12 weeks on a fully charged cell, and 4) 20 ºC for 16 weeks on a cell discharged to 4.0 V. After the storage period, cells were cycled at 1 mA/cm^2 and their performance was comparable to "as assembled" cells tested under an equivalent load. This data is presented in Figure 4. After varied storage conditions, the performance of the cell is observed with periodic deep discharge to 2.25 V during one of ten normal upper voltage (4.5 V to 3.5 V) cycles up until cycle 100. The data shows minimal changes in the peak location and shape, indicating a robust chemistry under various conditions. The differential capacity traces displayed in Figure 4 show the stability of the $Li_xMn_{2-y}Co_yO_{4-d}X_d$ cathode material when coupled with lithium in an electrochemical cell.

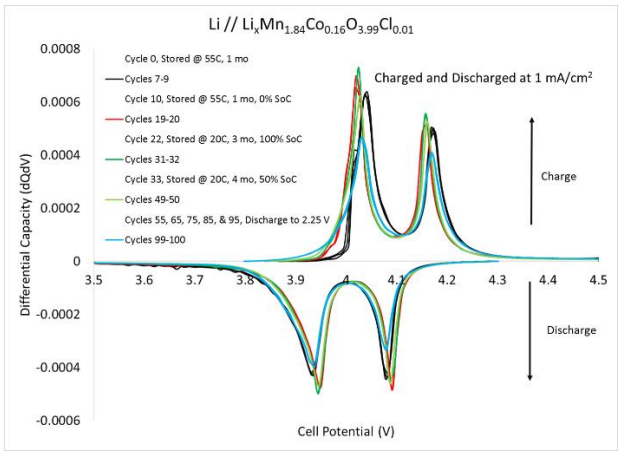

Figure 4. Galvanostatic data for a representative Li//$Li_xMn_{2-y}Co_yO_{4-d}X_d$ electrochemical cell subjected to repeated storage and subsequent deep discharge to 2.25 V.

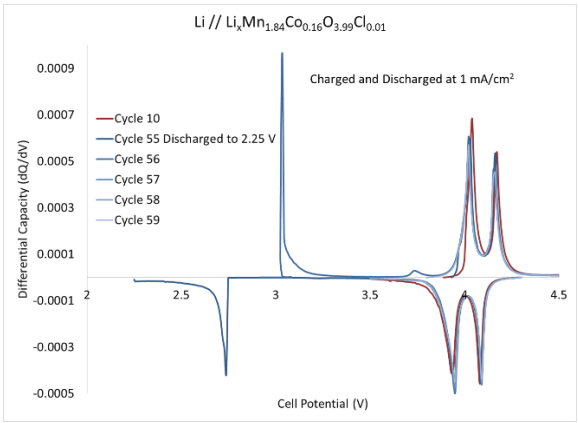

Figure 5. Galvanostatic data for a representative Li//$Li_xMn_{2-y}Co_yO_{4-d}X_d$ electrochemical cell showing thermodynamic stability.

Figure 5 displays the differential capacity traces for cycles 55-59 and compares them to cycle 10. This plot displays data for the same cell represented in Figure 4. No variations occurred between the deep discharge of cycle 55 and the consecutive cycles of 56 through 59. Cycles 56 through 59 also have very similar electrochemical behavior to cycle 10, even after the varied storage and cycling conditions. This

data further demonstrates the stability of the $Li_xMn_{2-y}Co_yO_{4-d}X_d$ cathode material.

Conclusion

A cobalt-doped lithium manganese oxide spinel with chlorine addition was synthesized. X-ray diffraction confirmed the proper AB_2O_4 lithium spinel phase was achieved successfully. The $Li_xMn_{2-y}Co_yO_{4-d}X_d$ spinel cathode material was incorporated into an experimental button cell opposite a lithium metal anode, and charge/discharge cycling was performed to determine the electrochemical performance of the novel cathode. The $Li//Li_xMn_{2-y}Co_yO_{4-d}Cl_d$ system demonstrated a low overpotential of 0.05 V in the 4.5 V to 3.5 V regime. Additionally, this chemistry yielded a very high specific capacity, nearing 240 mAh/g. After long term storage under various temperature conditions, the cell continued to exhibit the same electrochemical performance upon further cycling as compared with early cycle life performance. The stability of the chemistry was further demonstrated through periodic cycling to low voltage (2.25 V); the cell remained reversible upon recharging and continued to cycle under the 4.5 V to 3.5 V regime with equivalent capacity at extended cycling as compared to early cycling. These results demonstrate desirable traits for incorporation into lithium-ion batteries for the military.

References

1. David Linden (Ed.); Handbook of Batteries 4th ed.; McGraw-Hill, 2011
2. Tarascom, JM, Guyomard D, *J. Electrochem Soc.*, Vol. 138, Oct. 1991, pg. 2864
3. Thackeray MM, etal, Mater Res. Bull., 1984, pg 179
4. Gabano, JP, Lithium Batteries; Academic Press; New York, NY; 1983
5. Liu, W-R, et.al., *J. Power Sources*, 146 (2005) pg. 233-239
6. Kang, Y-J, et.al., *J. Power Sources*, 146 (2005) pg. 237-240
7. Kang, S-H, Goodenough JB, *J. Electrochem Soc.*, Vol. 147, No. 10, October 2000, pg. 3621-3627
8. Kang, S-H, Goodenough JB, *Electrochemical and Solid State Letters*, Vol. 3, No. 12, (2000), pg. 536-539
9. Sun, Y-K, et.al., *Electrochemical and Solid State Letters*, Vol. 3, No. 1, (2000), pg. 7-9
10. Inoue, T and Sano, M, *J. Electrochem Soc.*, Vol. 145, No. 11, November 1998, pg. 3704-3707
11. Larcher, D et.al.; *J. Electrochem Soc.*, Vol. 145, No. 10, October 1997, pg. 3392-3400
12. Wen, SJ et.al., *J. Electrochem Soc.*, Vol. 143, No. 6, June 1996, pg. L136-L138
13. Shao-Horn, Y et.al.; *J. Electrochem Soc.*, Vol. 144, No. 9, September 1997, pg. 3147-3153
14. Armstrong AR, et.al.; *J. Solid State Chem.*, Vol. 145, 1999, pg. 549-556
15. Yang, XQ et.al., *Electrochemical and Solid State Letters*, Vol. 2, No. 4, (1999), pg. 157-160
16. Xia, Y and Yoshio, M, *J. Electrochem Soc.*, Vol. 143, No. 3, March 1996, pg. 825-833
17. Xia, Y et.al., *J. Electrochem Soc.*, Vol. 148, No. 7, July 2001, pg. A723-A72
18. Terrill B. Atwater and Paula C. Latorre, Proceedings 46th Power Sources Conference, June 2014
19. Terrill B. Atwater and Paula C. Tavares, Proceedings 45th Power Sources Conference, June 2012
20. Terrill B. Atwater and Paula C. Latorre, SAE Int. J. Materials and Manufacturing. 6(1):2013 doi:10.4271 ISSN: 1946-3979, Jan. 2013
21. US Patent No. 8,900,756, Terrill B. Atwater and Paula C. Tavares, December 2, 2014
22. US Patent No. 8,597,377, Terrill B. Atwater and Paula C. Tavares, December 3, 2013
23. Filed Patent and Trademark Office SN: 14/636,183, Terrill B Atwater, Ashley L Ruth and Paula C Latorre, March 2015
24. Filed Patent and Trademark Office SN: 14/497,620,Terrill B. Atwater, Ashley L Ruth and Paula C Latorre, September 2014